THE PUBLISHING HOUSE
OF THE ROMANIAN ACADEMY

PROCEEDINGS OF THE ROMANIAN ACADEMY, Series A,
Volume 11, Number 2/2010, pp. 163–170

TRANSIENT THERMAL COUPLING FOR FLOWS OVER A FINITE THICKNESS PLATE EXPOSED TO A TIME-DEPENDENT TEMPERATURE

Emilia-Cerna MLADIN[1], Dorin STANCIU[1], Jacques PADET[2]

[1] "Politechnica" University of Bucharest, Dept. of Engineering Thermodynamics,
Spl. Independentei, 313, 060042, Bucharest, Romanie
[2] Universite de Reims, Champagne-Ardene, Laboratoire de Thermomecanique,
Moulin de la Housse B.P. 1039, 51687 Reims-France
Corresponding author: Emilia-Cerna MLADIN, E-mail: cerna_mladin@yahoo.fr

The aim of this work is to model the unsteady thermal boundary layer developing along a finite thickness plate under a ramp type variation of temperature on the bottom plate surface. The hydrodynamic boundary layer was considered laminar and at steady state. To model the transient heat transfer, two mathematical approaches were used: the integral method based on Karman-Polhausen methodology and the full Navier-Stokes system of equations, numerically solved with the commercial solver FLUENT. As a case study, a laminar water flow over a steel plate was considered, but the models remain valid for all combinations of incompressible fluids with $Pr > 0.7$ and solid materials. The results were expressed in terms of a deviation factor, defined as the ratio between the instantaneous heat flux associated with a finite thickness plate and the instantaneous heat flux associated with a zero thickness plate, both computed at the same space coordinate. Both methods were validated for steady state regime and zero plate thickness, by comparison with solutions commonly reported in the literature. The numerical results revealed that the two methods agree within 5% for the steady state and 2.6% for transient conditions.

Key words: Boundary layer flow; Transient convection; Thermal coupling; Ramp changes.

1. INTRODUCTION

Most of the previous works on heat convection in parallel flows over bodies use various boundary conditions at the contact surface. In all such cases, the plate thermal resistance is not encountered in calculus, although heat transfer may be highly influenced by the impact body geometry and material. In practical applications, however, it is most probably that the boundary conditions are known at the accessible surfaces, i.e. the ones that are not in contact with the flow. Use of common measuring instruments at the contact surface between the fluid and the body would clearly disturb the boundary layers and thus the measurements will be erroneous.

In the present paper, the authors aim to study the dynamics of the heat transfer in a parallel steady laminar flow over a finite thickness plate. The transient regime results from a ramp change in the temperature imposed at the bottom plate surface (the one that is not in contact with the fluid). Two mathematical approaches have been used for this purpose. One relies on a previously developed model [1, 2], based on the Karman-Pohlhausen integral methodology to formulate ordinary differential governing equations. The model was however modified to include a forcing function for the time-dependent boundary condition. The second approach uses the built-in finite volume conservation equations of the FLUENT code, that is based on the Patankar algorithms for incompressible flows [3]. The first model, although approximate to some extent, has the advantage of providing ordinary differential equations (ODS) that governs the system behavior. Such ODE's can then be easily integrated to study nonlinear dynamics effects associated with transients and embedded nonlinearities in the governing equations. The second approach is more accurate but the use of FLUENT code does not allow enough flexibility and hides the governing equations, making thus the embedded nonlinearities invisible.

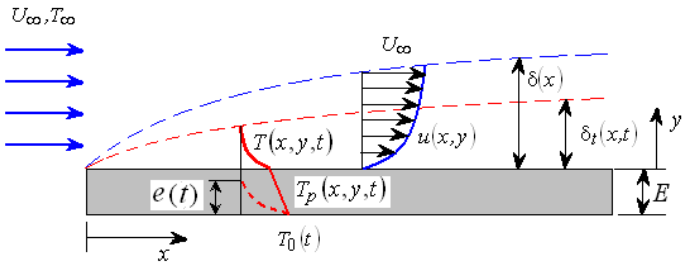

Fig. 1 – Description of the physical system.

Figure 1 schematically presents the physical system. The incompressible fluid flow is stationary and laminar and has a constant temperature T_∞. Its velocity U_∞ is constant as no pressure gradients are assumed. The flow is parallel with a plate of thickness E, which is much smaller than its length. The plate bottom surface temperature has an imposed temporal variation, $T_0(t)$. The initial state is of thermal equilibrium in the entire system. Therefore, when plate bottom surface temperature changes, the generated heat flux penetrates the plate and gives rise to a thermal boundary layer developing in the fluid. While the hydrodynamic boundary layer thickness $\delta(x)$ and velocity profile $u(x,y)$ are constant in time, the thermal boundary layer thickness $\delta_t(x,t)$ and temperature profile $T(x,y,t)$ are time-dependent as long as the transients last. The instantaneous temperature distribution within the plate $T_p(x,y,t)$ is distinctively illustrated in Fig. 1 for both the penetration phase (dotted line) and after penetration phase (solid line).

2. DESCRIPTION OF THE MODELS AND SOLUTION METHODOLOGIES

Momentum and energy conservation equations within the fluid domain, energy conservation equation only within the plate or solid domain, as well as the interface boundary condition growing from the energy equation are used in both approaches. The basic assumptions considered here for the heat transfer modeling are: (i) incompressible fluid with constant thermo-physical properties; (ii) negligible viscous dissipation (iii) $\delta_t \le \delta$ (Pr $\ge$ 0.7); (iv) constant plate thermal conductivity; (v) one-dimensional conduction and no heat sources within the plate. Let describe now the mathematical models of the two approaches.

2.1. Integral method

Let analyze first the flow and the convection heat transfer within the fluid domain. Under the above hypothesis, the integral forms of momentum and energy equations are:

$$\frac{\partial}{\partial x}\int_0^{\delta} u\left(u-U_\infty\right)\mathrm{d}y = -\nu \left.\frac{\partial u}{\partial y}\right|_{y=0}, \tag{1}$$

$$\frac{\partial}{\partial t}\int_0^{\delta_t}\left(T-T_\infty\right)\mathrm{d}y + \frac{\partial}{\partial x}\int_0^{\delta_t} u\ \left(T-T_\infty\right)\ \mathrm{d}y = a\left.\frac{\partial T}{\partial y}\right|_{y=0}, \tag{2}$$

In the above equations, ν represent the cinematic viscosity of fluid, a stands for its thermal diffusivity, while δ and δ_t denote the thicknesses of the hydrodynamic respective of the thermal boundary layers.

To obtain governing equations for δ and δ_t, time constant profile for velocity and temporally adaptive profile for temperature have to be specified. These profiles were modeled as high order polynomials, according to the Karman-Pohlhausen methodology. In dimensionless format and in connection to the boundary conditions, the fourth-order polynomial for the velocity and temperature profiles are [1, 5]:

$$u_* = u/U_\infty = 2\eta - 2\eta^3 + \eta^4, \qquad \eta = y/\delta, \tag{3}$$

$$\theta = \frac{T-T_\infty}{T_0^{ss}-T_\infty} = \theta_s - \left(2\theta_s + \frac{1}{3}\omega\right)\beta + \omega\beta^2 + +(2\theta_s - \omega)\beta^3 + \left(-\theta_s + \frac{1}{3}\omega\right)\beta^4, \qquad \beta = \frac{y}{\delta_t}. \tag{4}$$

In the above equation, the subscript *ss* stand for the steady state conditions, $\theta_s = \left(T_s - T_\infty\right)/\left(T_0^{ss} - T_\infty\right)$ is the dimensionless temperature at $y = 0$ (where $T = T_s$), and $\omega = \frac{1}{2}\left(x_* \,\mathrm{Pr}\,\Delta^2\right)\left(\partial\theta_s/\partial\tau\right)$ represents a time

dependent parameter depending on all, the stream-wise dimensionless coordinate $x_* = x/C^2$, the ratio of boundary layer thicknesses $\Delta = \delta_t / \delta$, the Prandtl number Pr, and the derivative of the surface temperature θ_s with respect to the dimensionless time $\tau = t \cdot \nu / C^4$. The mathematical expression of constant C will be specified later (see eq. 9). The time dependent polynomial coefficients allow the instantaneous adaptation of the temperature profiles to the transient thermal boundary conditions.

In the solid domain (within the plate), two distinct temporal phases were considered separately: (*i*) the initial phase of plate penetration, treated as conduction through a semi-infinite body with imposed thermal condition at $y = -E$, and (*ii*) after-penetration phase, associated with the thermal boundary layer development within the fluid (Fig. 1).

In the first phase, the penetration depth is $e(t) \le E$, meaning that $-E \le y \le -E + e(t)$. The integral form of energy equation is:

$$\frac{\partial}{\partial t}\int_{-E}^{-E+e} T_p(y)\cdot \mathrm{d}y - \frac{\partial e}{\partial t}\cdot T_p(-E+e) = a_s \cdot \left.\frac{\partial T_p}{\partial y}\right|_{-E}^{-E+e}. \tag{5}$$

The boundary conditions allow the plate temperature profile modeling as a third polynomial [6]:

$$\theta_p^i = \theta_0 - \left(\frac{3}{2}\theta_0 + \frac{1}{2}\omega_e\right)\cdot\frac{y+E}{e} + \omega_e \cdot \left(\frac{y+E}{e}\right)^2 + \frac{1}{2}(\theta_0 - \omega_e)\cdot\left(\frac{y+E}{e}\right)^3, \tag{6}$$

with $\theta_p = (T_p - T_\infty)/(T_0^{ss} - T_\infty)$. In this case, the time dependent parameter is $\omega_e = \frac{1}{2}(e_*^2 A \,\mathrm{Pr})(\partial\theta_0/\partial\tau)$ where $A = a/a_p$, is the ratio of fluid and plate diffusivities, $\theta_0 = (T_0 - T_\infty)/(T_0^{ss} - T_\infty)$ represents the instantaneous dimensionless temperature of the plate bottom surface (at $y = -E$), and $e_* = e/C^2$.

After the heat flux reaches the top plate surface (Fig. 1), the temperature boundary condition at $y = 0$, $\theta_p = \theta_S$ leads to a different temperature profile inside the plate [2]. The resulting polynomial is:

$$\theta_p = \theta_s + \left(\theta_s + \frac{2}{3}\omega_p + \frac{\mathrm{Pr}AE_*^2}{6}\theta_0^i - \theta_0\right)\frac{y}{E} + \omega_p\left(\frac{y}{E}\right)^2 + \frac{2\omega_p - \mathrm{Pr}AE_*^2\cdot\theta_0'}{6}\left(\frac{y}{E}\right)^3. \tag{7}$$

Now, $-E \le y \le 0$, and $\omega_p \equiv \frac{1}{2}(E_*^2 A\,\mathrm{Pr})(\partial\theta_s/\partial\tau)$, where $E_* = E/C^2$.

In order to close the model, some equations are needed from e, C, Δ, and θ_s. The differential equation governing the instantaneous penetration depth e has been derived by using the temperature profile (7) in the energy conservation integral equation (5), and has the form [1]:

$$\frac{\partial}{\partial\tau}\left(\frac{e_*}{E_*}\right)\left(6\theta_0 - \frac{e_*^2}{E_*^2}\mathrm{Pr}AE_*^2\frac{\partial\theta_0}{\partial\tau}\right) = \frac{24\theta_0}{\mathrm{Pr}AE_*e_*} - \frac{2e_*}{E_*}\frac{\partial\theta_0}{\partial\tau} + \frac{\mathrm{Pr}AE_*^2}{3}\left(\frac{e_*}{E_*}\right)^3\frac{\partial^2\theta_0}{\partial\tau^2}. \tag{8}$$

The penetration time is calculated from the above equation and corresponds to the condition $e = E$.

The use of polynomial (3) in the fluid momentum integral equations (1) leads to the hydrodynamic boundary layer thickness:

$$\delta = 5.83\sqrt{\nu \cdot x / U_\infty} = C\sqrt{x}. \tag{9}$$

For the energy conservation equation within the fluid and the interface boundary condition, two more assumptions have been made in addition to the temperature profile (4):

(i) the thermal boundary layer thickness varies with the spatial coordinate x in a similar way as the hydrodynamic boundary layer thickness; it results that their ratio is x-independent, $\Delta(\tau) \equiv \delta_t(x,\tau)/\delta(x,\tau)$;

(ii) the temperature distribution within the fluid may be expressed as a product between the steady-state solution and a transient deviation factor, by using the variable separation, $\theta_S(x,t) = \theta_S^{ss}(x)\cdot\theta_S^t(t)$. In this way, the spatial coordinate x is decoupled and the resulting governing equations for the fluid domain are ordinary differential equations with respect to time only.

The equation of Δ is obtained by introducing the polynomial profile **(4)** in the energy equation **(2)**. It has the following form:

$$\frac{\partial\Delta}{\partial\tau}\left(\frac{3}{10}\theta_s-\frac{1}{40}x_*\,\mathrm{Pr}\,\frac{\partial\theta_s}{\partial\tau}\Delta^2\right)=\frac{\theta_s}{x_*}\left[\frac{2}{\mathrm{Pr}}\frac{1}{\Delta}-\frac{5{,}83^2}{2}\left(2-\theta_s^{ss}\right)\Delta\cdot\varphi_1\right]+$$
$$+\left[\frac{5.83^2}{4}\mathrm{Pr}\left(4-\theta_s^{ss}\right)\Delta^3\varphi_2-\frac{2}{15}\Delta\right]\frac{\partial\theta_s}{\partial\tau}+\frac{x_*\,\mathrm{Pr}}{120}\Delta^3\cdot\frac{\partial^2\theta_s}{\partial\tau^2}. \tag{10}$$

The combination of heat flux boundary condition $k\left(\partial\theta_s/\partial y\right)_{y=0}=k_p\left(\partial\theta_p/\partial y\right)_{y=0}$ at the solid-fluid interface with the polinomial temperature profiles (4) and (7) leads to the following equation of θ_s:

$$\frac{\mathrm{d}\theta_s}{\mathrm{d}\tau}\left(2+\frac{\Delta\sqrt{x_*}\Lambda}{AE_*}\right)=\frac{6}{\mathrm{Pr}\,AE_*^2}\left[\left(\theta_0-\frac{1}{6}\mathrm{Pr}\,AE_*^2\cdot\frac{\mathrm{d}\theta_0}{\mathrm{d}\tau}\right)-\theta_s\left(\frac{2\Lambda\cdot E_*}{\Delta\cdot x_*}+1\right)\right], \tag{11}$$

where $\varphi_1=2/15\cdot\Delta-3/140\cdot\Delta^3+\Delta^4/180$, $\varphi_2=\Delta/90-\Delta^3/420+\Delta^4/1512$ and $\Lambda=k/k_p$ is the ratio of fluid and plate thermal conductivities. It is remarkable that the governing eqs. (10) and (11) are coupled and highly nonlinear. The steady-state forms and solutions are readily obtained by canceling the time-derivatives.

The transient solutions were obtained by integrating the ordinary differential equations by Runge-Kutta algorithms of fourth and fifth order. The integration was performed with different time steps, depending on the variable time responses. Most commonly, very small time steps were used at the beginning, due to the rapid increase of the thermal boundary layer thickness. The subsequent system dynamics allowed for larger time steps and thus for reasonable computational durations. The singularities present at $\tau=0$ were avoided by considering limiting values for Δ and θ_S.

Temperature polynomial profiles are illustrated in Fig. 2a, next to those obtained with the aid of FLUENT code. The temporal variation of boundary function $\theta_0(\tau)$ is presented in the bottom panel. This function is mathematically defined by eq. (18). The resulting temperature distributions within the plate and in the thermal boundary layer are shown in the midle and in the top panels. Here, the dotted lines represent the temperature variations during the penetration phase and the broken line sugests the corespondence between the temperature profiles within the solid and the fluid domains.

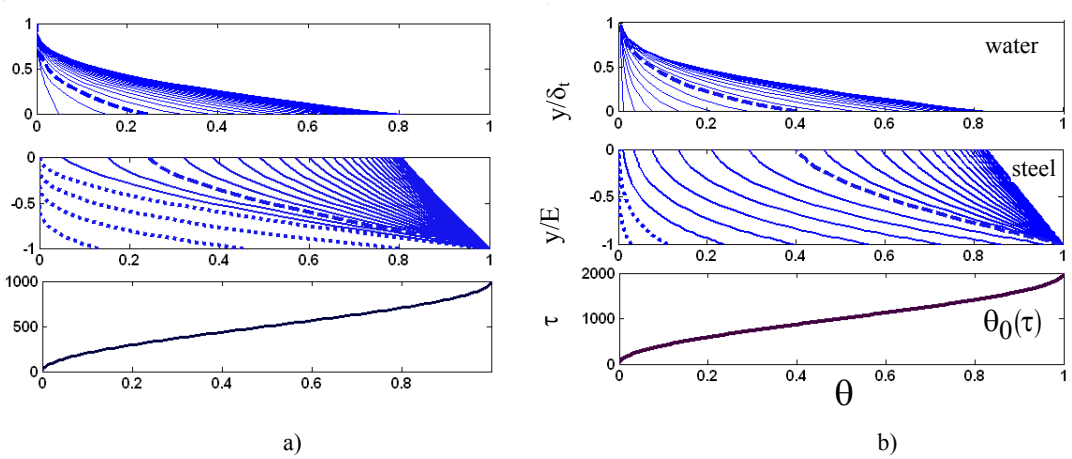

Fig. 2 – The comparison of temperature profiles obtained from integral and numerical simulation approaches: a) temperature polynomial profiles; b) temperature profiles with FLUENT.

2.2. Finite-volume approach

This second method uses the full formulation of differential conservation equations expressed in the physical variables. The fluid flow and the convective heat transfer in the boundary layer domain is modeled by the continuity, momentum and energy equations [10, 11]:

$$\frac{\partial}{\partial x_j}\left(\rho u_j\right)=0\,;\qquad \frac{\partial}{\partial x_j}\left(u_i u_j+\frac{p}{\rho}\delta_{ij}-\nu\frac{\partial u_i}{\partial x_j}\right)=0\,;\qquad \frac{\partial T}{\partial t}+\frac{\partial}{\partial x_j}\left(u_j T-a\frac{\partial T}{\partial x_j}\right)=0\,. \tag{12-14}$$

In the solid domain, only the energy equation is needed:

$$\frac{\partial T_p}{\partial t}+\frac{\partial}{\partial x_j}\left(a_p\frac{\partial T_p}{\partial x_j}\right)=0\,. \tag{15}$$

Note that, under the general assumption presented in the second paragraph, the momentum and energy equations are uncoupled. It follows that it can be solve first only the flow equations, which are steady state and after that, the time dependent energy equations in both fluid and solid domains.

On the bottom surface of the plate, the imposed boundary condition is $T_0=T_0(t)$ (see eq. 18). As pointed out above, its particular form used in this work will be specified later, in the fourth paragraph. At the fluid-solid interface, the no-slip boundary conditions and the continuity of the transferred heat flux $q_s= k\left(\partial T_s/\partial y\right)_{y=0}=k_p\left(\partial T_p/\partial y\right)_{y=0}$ were used to derive the velocity and temperature profiles.

The numerical solutions were obtained with the commercial code FLUENT 6.0.12 [11]. This solver code provides many spatial and temporal discretization procedures, which can be selected according to the particular case under consideration. Thus, there were employed here the second order upwind scheme for the spatial discretization of momentum and energy equations, and the PISO algorithm with neighbor correction for the pressure correction equation. The temporal discretization of energy eqs. (14–15) was performed with Euler second order implicit scheme.

The initial solution was obtained by a steady state calculation for an isothermal boundary layer flow developed on the finite thickness flat plate. Once the time-dependent thermal boundary condition $T_0(t)$ was set at the plate bottom surface ($y=-E$ in Fig. 1), the unsteady calculation was performed and transient solutions resulted. For the particular case of a step change in the surface temperature, the grid independency on the numerical solution was obtained through the grid adaptation technique of the initial mesh at the solid-fluid boundary interface. Then, the same mesh was used for all other calculations.

Figure 2b illustrates the temperature profiles within the fluid as well as within the plate, as obtained with the finite-volume approach and FLUENT code. As in previous case, the dotted lines represent the temperature variations during the penetration phase and the broken line sugests the corespondence between the temperature profiles within the solid and the fluid domains. Note also that there is any link between the broken lines appearing in the middle panels of the two approaches.

3. HEAT TRANSFER PERFORMANCE

This study analyzes the transient heat transfer performances in parallel flows over a flat plate. Most of the correlations reported in the literature do not consider the conduction through the plate, or, otherwise said, consider the plate of zero thickness and impose a condition (e.g. temperature or heat flux) at the contact surface. However, real situations deal with finite thickness plates, $E\neq 0$. Then, the surface temperature varies along the plate and the local Nusselt number ($\equiv hx/\lambda$) used to compute the local heat transfer coefficient h, becomes insufficient for using the Newton's law $q_s\left(x\right)=h\left(x\right)\left[T_s\left(x\right)-T_\infty\right]$. In order to point out the impact plate influence on the heat transfer, a deviation factor, DF, is defined as the ratio between the instantaneous heat flux associated with a finite thickness plate and the instantaneous heat flux associated with a zero thickness plate, both at the same spatial location. The surface heat flux is easily obtained from the Fourier's law and the temperature profile within the thermal boundary layer. The integral method provides the following expression based on eq. (4):

$$\mathrm{DF}\equiv\frac{q_s\left(E\neq 0\right)}{q_s\left(E=0\right)}=\left(\theta_s+\frac{\omega}{6}\right)\frac{\Delta\left(E=0\right)}{\Delta\left(E\neq 0\right)}. \tag{16}$$

For a finite thickness plate, the interface temperature θ_S is always inferior to unity. As time goes to infinity, the deviation factor reaches its steady-state value ($\omega=0$), which is also inferior to unity:

$$DF^{ss} = \theta_s^{ss} \frac{\Delta^{ss}(E=0)}{\Delta^{ss}(E\neq 0)} < 1 \tag{17}$$

Knowledge of the steady-state deviation factor would allow the use of the present correlations derived for a zero thickness and isothermal impact plate.

4. SELECTED FORCING FUNCTION AND SYSTEM PARAMETERS

In the present study, the temperature imposed at the plate bottom surface will follow a temporal ramp variation of finite duration. The step change may be viewed as a limiting case, i.e., a ramp of zero duration. This type of forcing function has been chosen as it models the real variations which are never totally abrupt. However, the developed models can be used with any other temporal variation of the imposed boundary condition so long as the variations are piece-wise smooth.

The ramp function is characterized by its duration D. In dimensionless variables, it starts from an initial value of zero, corresponding to thermal equilibrium, and a final value of unity associated with the steady-state conditions:

$$\theta_0 = \begin{cases} \frac{1}{2}\left[1+\sin\left(\frac{\pi\cdot\tau}{D}-\frac{\pi}{2}\right)\right] & , \quad 0 \le \tau < D \\ 1 & , \quad \tau \ge D \end{cases} \tag{18}$$

The ramp profile is presented in Fig. 2, in the bottom panels. Solutions were obtained for various system parameters but will be reported here only for an illustrative case: water flow over a steel plate. The inflow velocity was chosen U_∞=1 m/s. However, the two models may be equally used for other combinations of fluids and solids, as long as the fluid Prandtl numbers are greater than 0.7.

5. MODEL VALIDATION

Under steady-state conditions and zero plate thickness, the integral method provided the following expression for the Nusselt, as derived from its definition:

$$\mathrm{Nu}_x \equiv \frac{hx}{k} = 0.343\,\mathrm{Re}_x^{1/2}\,\frac{1}{\Delta^{ss}}, \tag{19}$$

where $h \equiv -k(\partial T/\partial y)_{y=0}/(T_S - T_\infty)$.

On the other hand, the Fluent code provided values for the same Nusselt numbers. All values were validated against other solutions previously reported for steady-state conditions and a zero thickness plate. Particular values and associated errors are shown in Table 1.

Table 1

Some steady state solution for zero plate thickness and their errors for $x^* = 7000$, Re_x=237922

Correlation	Relation	Value and relative error
Exact solution [9]:	$\mathrm{Nu}_x \equiv \frac{hx}{k} = 0.332\,\mathrm{Re}_x^{1/2}\,\mathrm{Pr}^{1/3}$	309.774 **0%**
Integral solution [8]:	$\mathrm{Nu}_x \equiv \frac{hx}{k} = 0.343\,\mathrm{Re}_x^{1/2}\,\mathrm{Pr}^{1/3}$	320.038 **3.3%**
Present integral solution	Equation (19), $E* = 0$, $\Delta^{ss} = 0.5076$ for Pr = 0.7	329.600 **6.4%**
Fluent code	Numerical simulation	311.013 **0.4%**

The assumption that the boundary layer thickness ratio Δ is not a function of x_* in eq. (10) was checked for x_*=1000 – 13000 and a plate thickness $E* = 100$. The steady-state values of Δ^{SS} ranged from 0.4576 to 0.4875, which leads to an interval error of 6.2%.

The error levels of less than 6.5% rend the methodologies used here appropriate for engineering applications. The steady-state error analysis confers credibility to the transient solutions used further to characterize the instantaneous heat transfer performance and which cannot be compared to other previously reported results.

6. RESULTS

Under transient conditions, Fig. 3 illustrates the surface temperature dynamics for different ramp durations and for both methods. It appears that the major differences occur in the penetration times, they being much smaller when calculated with FLUENT solver. This result may be attributed to the 3rd polynomial profile imposed for the plate temperature during the penetration time, as well as to singularities encountered in the governing differential equations (10) and (11) when the thermal boundary layer starts developing.

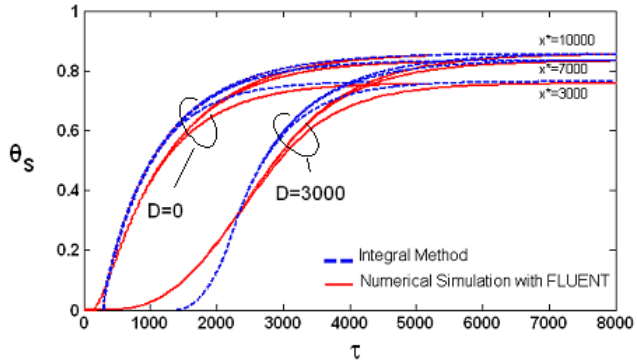

Fig. 3 – Surface temperature dynamics for two ramp durations and three x-locations.

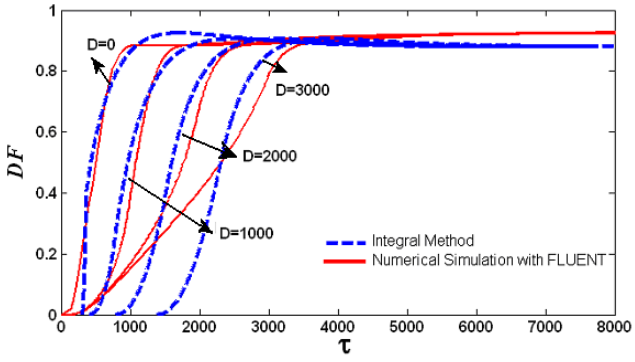

Fig.4 – Deviation factor DF for the different ramp durations and x_* = 7000.

The influence of the impact plate on the heat transfer performance represents the most significant aspect of the problem. As stated earlier, results were expressed as a deviation factor *DF* defined in eq. (16). In this way, the influence of thermal coupling is indicated by the difference between the *DF* value and unity. The comparison of the two types of solutions is shown in Fig. 4 for different ramp durations in the forcing function of θ_0 and for the location x_* = 7000. The results indicate that all the DF-values are inferior to unity even under steady-state conditions. However, the FLUENT code provided a value (DF = 0.9228) that is 4.7% higher that that obtained with the integral method (DF=0.8791).

The maximum zones (bumps) indicated at the end of transients derive from the fact that during the penetration times, there is a heat flux to the fluid for the zero-thickness plate but no heat transfer for the finite-thickness plate. Equation (16) indicates that DF depends on the ratio of the boundary layer thicknesses associated with E = 0 and $E \neq 0$, respectively. This ratio is obviously higher than unity during the penetration times and induces also higher values afterwards. The "bumps" are shown to decrease as the ramp duration increases and have lower values at more remote locations from the plate leading edge.

Under transient conditions, the instantaneous differences are significant, especially due to the high penetration times related to the integral approach. However, even shifted in time, the DF-growths deduced from this method are more abrupt, rapidly approaching the steady-state values. Table 2 presents the time-averages of the deviation factor for the curves of Fig. 4. Transient time was defined as the time needed to reach 95% of the steady-state value.

Table 2

Time averaged of DF for different values of D

Ramp duration (eq.11)	$D = 0$	$D = 1000$	$D = 2000$	$D = 3000$
Present integral method	0.8226	0.7064	0.6617	0.6011
FLUENT	0.8425	0.7057	0.6741	0.5855

Results indicate that the time-average differences between the two approaches range from –2.4% for the step change in T_0 ($D = 0$) to 2.6% for a ramp change of duration $D = =3000$. If the transient time is redefined, i.e. the time needed to reach 90% or 99% of the steady-state value, the time-averages diminish or increase accordingly.

6. CONCLUSION

The study aimed to characterize the unsteady heat transfer performance in the case of a parallel laminar and stationary flow over a finite thickness plate. Two methodologies were applied: a semi-analytical one based on the integral approach of Karman-Pohlhausen, and a numerical simulation using the finite-volume descretization of the system domain with the aid of the FLUENT commercial solver. Both methods were validated against results previously reported for a zero-thickness plate and stationary conditions.

The paper presents an illustrative case of a water flow of 1 m/s incident velocity over a steel plate, 0.4 m long and 3.4 mm thick. The forcing function was chosen to be a ramp change in the temperature imposed at the plate surface that is not in contact with the fluid.

The interface temperature was shown to significantly vary with the spatial coordinate parallel to the plate, fact that does not allow anymore the simple use of a Nusselt number correlation for the heat transfer rate calculus. For this reason, the heat transfer results were reported as a deviation factor defined as the ratio of the heat flux associated with the finite thickness plate and the heat flux associated with the zero thickness plate. In this way, two aspects are addressed: first, the departure of the deviation factor from unity indicates the plate influence on the heat transfer performances; second, the current correlations derived for a zero thickness plate can still be used and then corrected with the deviation factor as indicated here.

Results related to the deviation factor dynamics indicated that the two methods agree within 5% under steady-state conditions, and within 2.6% for the transients, with higher differences for ramps of higher durations.

The numerical solutions indicated the magnitude of the impact plate influence on the heat transfer performances as compared to the zero thickness plate. For example, for a ramp change of $D = 3000$ (3 s), the deviation factor had a time-average of about 0.59, meaning 41% less heat transferred to the fluid during the transient regime. This result suggests that for frequent changes (on-off regimes) in the applied temperature, or for longer ramps, the neglecting of the plate influence could lead to great errors in the engineering application design or operation.

REFERENCES

1. MLADIN, E.C., RĂDULESCU M., *Thermal Convection in Parallel Flows over a Finite Thickness Plate and Ramp Temperature Change*, Proceedings of BIRAC'02, pp. 115–124, 2002.
2. MLADIN, E.C., LACHI M., PADET J., *Transfert de chaleur couplé conduction-convection en régime instationnaire, induit par une temperature imposée sur une plaque d'épaisseur finie*, Congres Francais de Thermique, SFT Nantes, 87–92, 2001.
3. PATANCAR V.S., *Numerical Heat Transfer and Fluid Flow,* Hemisphere Publishing Corp. New York,1980.
4. MLADIN E.C., PADET J., *Unsteady planar stagnation flow on a heated plate*, Int. J. of Thermal Sciences, **40**, *7*, pp. 638–64, 2001.
5. MLADIN E.C., RĂDULESCU M., REBAY M., PADET J., *Transient thermal convection in a parallel flow over a finite thickness plate and an isothermal surface*, Travaux du Colloque Franco-Roumain COFRET'02, Bucarest, 2002 pp. 326–334.
6. ÖZIŞIK M.N., *Heat Conduction*, 2nd Edition, John Wiley &Sons, Inc., New York, 1993.
7. LECA A., MLADIN E.C., STAN M., *Transfer de caldura si masa*, Edit. Tehnică, Bucureşti, 1998.
8. PADET J., *Principes du transfert convectifs*, Ed. Polytechnica, Paris, 1998.
9. SCHLICHTING H, *Boundary Layer Theory*, McGRAW-HILL, 1960.
10. CONSTANTINESCU V.N., *Dynamics of viscous fluids in laminar flow*, Edit. Academiei Române, 1987.
11. *** *User's guide v6.012*, FLUENT inc., Lebanon USA, 2001.

Recived October 29, 2009